E|DPC-2015

Electric Drives Production Conference 2015

2015 5th International Conference

Electric Drives Production

September 15th – 16th, 2015
Nuremberg, Germany

Proceedings

MARSILLI

IEEE
VDMA Antriebstechnik
mesago Messe Frankfurt Group
E|Drive-Center Bayerisches Technologiezentrum für elektrische Antriebstechnik

2015
5th International
Electric Drives Production
Conference (E|DPC)

September 15th - 16th, 2015
Nuremberg, Germany

Proceedings

IEEE Catalog Number: CFP1585P-PRT
ISBN: 978-1-4673-7511-5

2015 5th International Electric Drives Production Conference (E|DPC)

Influence of Production Uncertainties and Operational Conditions on Torque Characteristic of an Induction Machine

G. von Pfingsten, M. Hombitzer, and K. Hameyer *Senior Member IEEE*

Institute of Electrical Machines (IEM)
RWTH Aachen University
52062 Aachen, Germany
post@iem.rwth-aachen.de

***Abstract*—The influence of production uncertainties in torque characteristics is evaluated by off line and extensive test bench measurements of ten induction machines from series production. Adapting a machine model to each of the individual machines allows to analyze the deviation of the test bench results.**

Keywords — Electrical Machines, Production Uncertainty, Torque Deviation, Torque Accuracy, Electric Vehicle

I. Introduction

The influence of uncertainties on torque characteristics due to series production on the operational behavior of an induction machine (IM) is studied. Measurements under identical test conditions are conducted for a series of motors. The input of the inverter is the requested torque. The difference in behavior between ten machines from two series batches is studied by measurements. Rotor and stator temperatures are recorded for all machines. The influence of production uncertainties and uncertainties in operation conditions influence the machine behavior of each individual machine. Ten machines are measured individually and the measured results are analyzed to find the influence of uncertainties from production and operation. This is achieved by adapting a nonlinear fundamental wave model to the test bench measurements of each machine.

II. Motivation

Modular drive train systems offer the advantage of using multiple identical parts. This may lead to lower production cost and higher reliability.

These 'identical' parts are subject to uncertainties from production and operation. Reality shows that they do not have identical properties.

The studied drive train consists of two inverters and two 15 kW four pole IMs, which drive the rear wheels of an electric vehicle independently. This modular propulsion system offers the possibility to apply different torque values to each of the wheels and increase driving performance as well as safety [1]. However, producing a torque differing from the requested torque would lead to worse comfort and reduced driving safety.

Most of the publications regarding production uncertainties of electrical machines concentrate on modeling parasitic effects such as eccentricity harmonics [2,3], body-sound [4], and torque ripple [5,6]. In [7] the starting currents of multiple IMs are measured and analyzed.

In contrast, this paper analyzes the influence of production uncertainties on torque characteristics (in particular torque accuracy).

III. The Studied Machine

The studied machines are designed as traction drives for small electric vehicles. The ten individual machines come from two series batches. The second batch was produced a few months after the first batch. Stator and rotor core are produced by punching. The rotor cage consists of die casted aluminum. Fig. 1 shows the cross section of the machine.

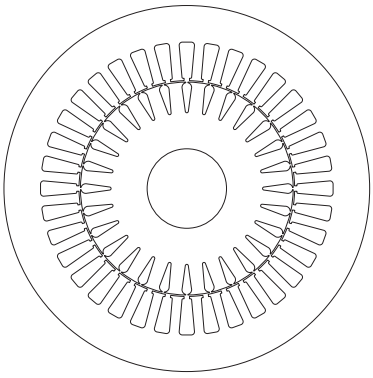

Fig. 1: Cross section of the studied machine.

IV. Off Line Measurements

The stator resistance between each of the terminals (U, V, W) is determined by four-terminal-sensing at room temperature (Fig. 2). Since the difference between the three measured resistances of each machine is small, the highest difference of the average of the three measured resistances per machine is with 1.36 % (min: 11.01 mΩ, max: 11.16 mΩ) only little bit smaller than the highest difference of all measured values (1.53 %, min: 11.00 mΩ, max: 11.17 mΩ).

The rotor outer diameter and stator bore diameter are measured using an outside micrometer and a three point micrometer respectively. The diameters are measured at three axial positions (front, middle, end) and two tangential positions (0°, 90°). From the diameters the average air gap is calculated (Fig. 3). The average air gap of all machines is 0.478 mm. The

978-1-4673-7512-2/15/$31.00 ©2015 IEEE

machine with the largest air gap width (0.485 mm) has about 3.2 % larger air gap when compared to the machine with the smallest air gap (0.47 mm).

The dynamic eccentricity caused by inaccuracy of the last step of the rotor production process (turning on lathe) and by the bearings is identified using a dial test indicator whilst slowly turning the rotor by hand. This eccentricity is smaller than 0.02 mm. However the additional dynamic eccentricity caused by bending vibrations because of rotor unbalance could not be measured directly. Hence axial and radial surface acceleration was measured in six identical positions on each housing of the machines in a full load run up test (0 → 7500 min^{-1}). Since no significant difference in the acceleration values was found the dynamic eccentricity is assumed to be small.

A 2D FEM model of the machine is employed to find the influence of dynamic eccentricity and air gap width on the torque characteristic of the machine. The found influence of these geometric parameters is 0.65 % at the maximum torque operation.

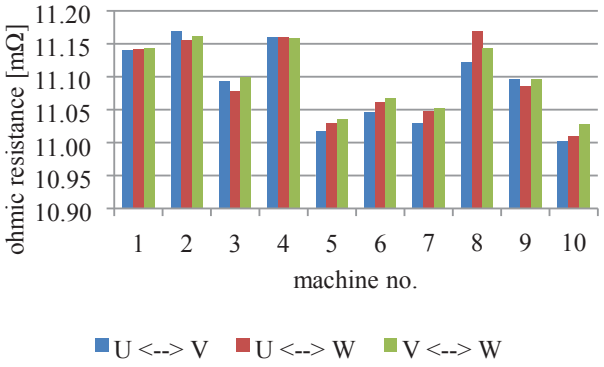

Fig. 2: Measured stator resistance.

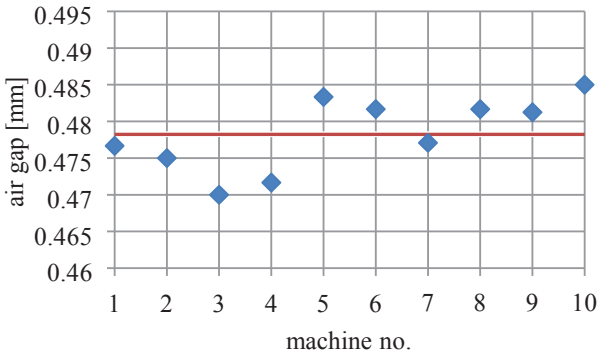

Fig. 3: Air gap width from measurements of stator bore diameter and rotor outer diameter.

V. Test Bench Measurements

A. Measurement setup

The IMs are designed for an electric vehicle and feature only one bearing. In the application the second bearing is located in the gear. A custom bearing shield was built to support the rotor on the second side. This custom bearing shield was fitted with an infrared (IR) temperature sensor which is focused on the short circuit ring. The rings were spray-painted black. The winding temperature is measured by the inverter.

One additional machine with four rotor temperature sensors (Pt-100) and six Pt-100 sensors in the stator winding was measured to verify the IR rotor temperature measurement and the inverters winding temperature measurement.

200 operating points (n,T_{req}) at equal speed (n) and requested torque (T_{req}) values were driven and measured for every machine (m = 1 … 10). The three phase voltages and currents are measured using a power analyzer. From these voltages and currents the three phase electrical active and reactive power and the power factor are analyzed. The losses in the machine $P_{loss,\,meas}$ are calculated as difference of the three phase active power $P_{3ph,\,meas}$ and the mechanical power $P_{mech,\,meas}$ according to (1).

$$P_{loss,\,meas}(m,n,T_{req}) = P_{3ph,\,meas}(m,n,T_{req}) - P_{mech,\,meas}(m,n,T_{req}) \quad (1)$$

Since the rotor temperature highly effects the characteristics of the IM, it was kept in a range of 100 °C to 125 °C during all measurements. The measured stator winding temperature ranged from 60 °C to 130 °C.

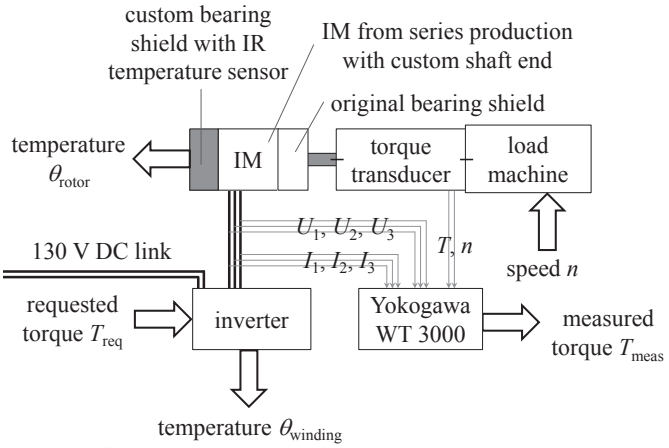

Fig. 4: Configuration of the test bench.

B. Results of Measurements

The difference between measured torque T_{meas} and required torque T_{req} in all operating points (n,T_{req}) is calculated for each machine m. Fig. 5 shows the mismatch of measured and requested torque as average value of all ten machines (M = 10) as defined in (2). The highest absolute torque mismatch of more than 6 Nm is found at the highest torque value of 120 Nm and rated speed. In this operating point the machines produce 6 Nm less torque than requested. At a speed of 4000 min^{-1} to 6000 min^{-1} and maximum power the machines produce in average about 2 Nm more torque than requested.

$$\Delta T(n,T_{req}) = \frac{1}{M}\sum_{m}[T_{meas}(m,n,T_{req}) - T_{req}] \quad (2)$$

To quantify the deviations between the test bench measurements of the machines in terms of torque, the difference

between average measured torque and each measurement point is evaluated using the standard deviation σ_{meas} (3).

$$\sigma_{\text{meas}}=\sqrt{\frac{1}{M}\sum_{m}[T_{\text{meas}}(m,n,T_{\text{req}})-\bar{T}_{\text{meas}}(n,T_{\text{req}})]^2}$$
$$\bar{T}_{\text{meas}}(n,T_{\text{req}})=\frac{1}{M}\sum_{m}T_{\text{meas}}(m,n,T_{\text{req}}) \quad (3)$$

Fig. 6 shows the deviation σ_{meas} between the machines over the full torque speed range. The highest deviation ($\sigma_{\text{meas}} \approx 1.6$ Nm $\widehat{=}$ 2.5 %) between the machines is measured at the speed of 4500 min^{-1} and maximum power. At the maximum torque, σ_{meas} is approx. 0.8 Nm ($\widehat{=}$ 0.7 %). These values meet the specified maximum torque difference for the application of the studied drive train. However, other applications might need a higher absolute torque accuracy or less torque deviation between two drives.

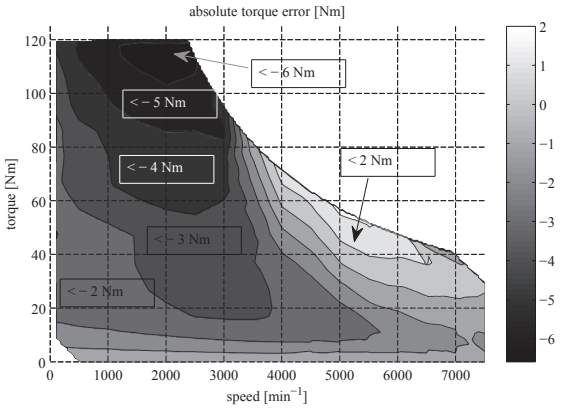

Fig. 5: Difference between requested and delivered torque ΔT as defined in (2).

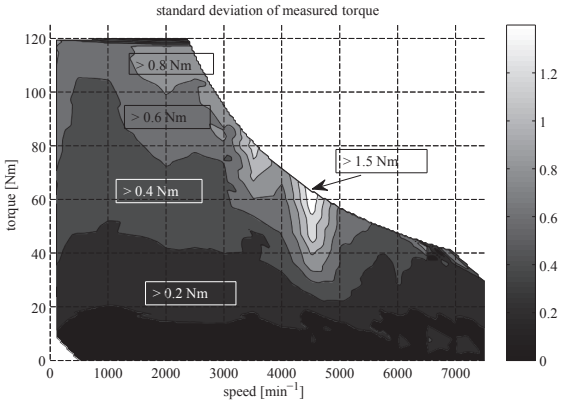

Fig. 6: Standard deviation σ_{meas} of measured torque as defined in (3).

VI. Adaptation of Machine Model

From the 200 measured operating points a fundamental wave machine model is parametrized for each of the machines. The standard T-electric equivalent circuit (Fig. 7) is used. The operating point depending resistance R_{Fe} representing the iron losses is assumed in parallel to the main and stator stray inductance to reduce the influence of $L_{\sigma,1}$ and I_1 on estimating R_{Fe}. This makes the model more stable.

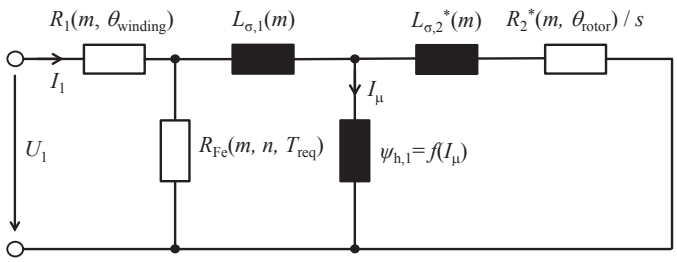

Fig. 7: Electric equivalent circuit.

Measured winding temperature θ_{winding} and measured rotor temperature θ_{rotor} are used to compensate for the influence of temperature on stator and rotor resistance. The input of the model are the measured values of

- stator voltage: U_1,
- rotor speed: n,
- frequency of stator currents: f_1,
- temperature of rotor end ring: θ_{rotor}, and
- temperature of winding: θ_{winding}.

From these input parameters the output values

- torque: T_{model},
- stator current: $I_{1,\text{model}}$,
- power factor: Λ_{model}, and
- losses: $P_{\text{loss, model}}$

are calculated for every of the 200 measured operating points and every machine using the parameter set S. S consists of the measured stator resistance from Fig. 2,

- stator stray inductance: $L_{\sigma,1}$,
- rotor stray inductance: $L^*_{\sigma,2}$,
- rotor resistance: R^*_2, and
- nonlinear main flux linkage: $\psi_{\text{h},1}=f(I_\mu)$.

Fig. 8 shows one nonlinear magnetization curve. The main flux linkage is scaled to transform the saturation flux linkage to a degree of freedom in the model. One parameter set S has four degrees of freedom which are found by evaluating a quality function. For every of the four degrees of freedom a parameter range was set. A four-dimensional (4D) space is created by these ranges. The model is evaluated for every combination S of the 4D space and every measured point (m,n,T_{req}). Since the main inductance is nonlinear, the value of the main flux and main inductance are found through iteration in every simulated point. Given that the main flux linkage is strictly monotonic increasing with the magnetization current I_μ, a good convergence of the nonlinear main flux linkage is attained. The model depicted in Fig. 7 is stable in all operating points.

Saturation harmonics are analyzed using a 2D nonlinear FEM model of the machine. In normal operation, i.e., with a main flux linkage smaller than 0.12 Vs the influence of saturation harmonics on the machine behavior is small and therefore the fundamental wave model is applicable.

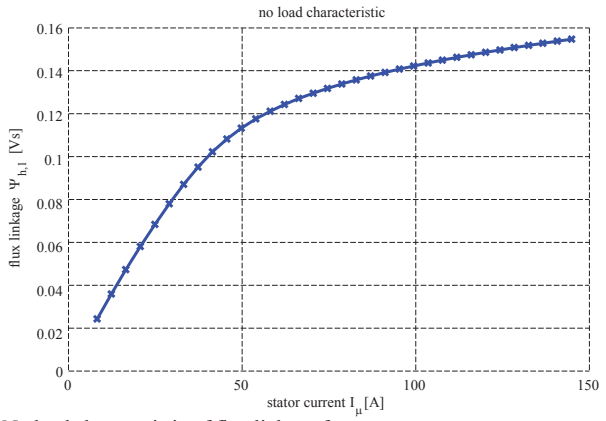

Fig. 8: No load characteristic of flux linkage from measurement.

The model error e defined in (4) is used as the quality function to find each parameter set S_m which describes the characteristic of each machine m the best, i.e. $e(m,S_\mathrm{m})\rightarrow\min$. To avoid a large influence of possible errors in one measured variable, the five largest squared errors (of the 200) in each category (T,P,Λ, and I_1) are set to the sixth largest value in the concerned category.

$$e(m,S_\mathrm{m}) = \sum_{n,T_\mathrm{req}} \left[\frac{T_\mathrm{model}(m,n,T_\mathrm{req},S_\mathrm{m})-T_\mathrm{meas}(m,n,T_\mathrm{req})}{\max(T_\mathrm{meas})}\right]^2 \left[\frac{P_\mathrm{loss,\,model}(m,n,T_\mathrm{req},S_\mathrm{m})-P_\mathrm{loss,\,meas}(m,n,T_\mathrm{req})}{\max(P_\mathrm{loss,\,meas})}\right]^2 + \left[\frac{\Lambda_\mathrm{model}(m,n,T_\mathrm{req},S_\mathrm{m})-\Lambda_\mathrm{meas}(m,n,T_\mathrm{req})}{\max(\Lambda_\mathrm{meas})}\right]^2 + \left[\frac{I_\mathrm{1,model}(m,n,T_\mathrm{req},S_\mathrm{m})-I_\mathrm{1,meas}(m,n,T_\mathrm{req})}{\max(I_\mathrm{1,meas})}\right]^2 \quad (4)$$

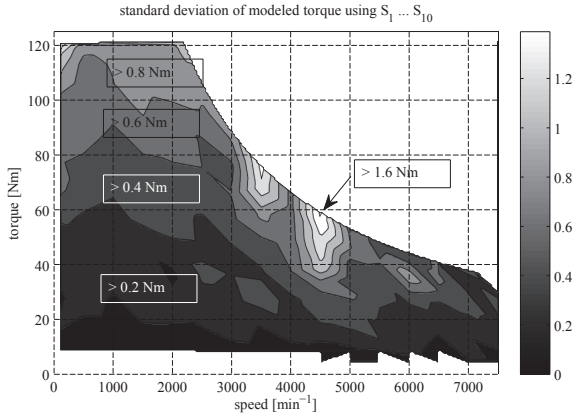

Fig. 9: Standard deviation σ_a of modeled torque using parameter sets S_1 … S_{10}.

From the m fitted parameter sets the modeled torque T_model is calculated for each measured operating point. The standard deviation from (5) is used to quantify the torque differences in the model (Fig. 9). The measured and modeled torque deviation (Fig. 6 and Fig. 9) differ less than 0.1 Nm in most operating points. The model with the ten individual parameter sets simulates the measured behavior well. The model parameter sets $S_1 \ldots S_{10}$ contain the identified uncertainties from the test bench measurements.

$$\sigma_\mathrm{a}=\sqrt{\frac{1}{M}\sum_m [T_\mathrm{model}(S_\mathrm{m},m,n,T_\mathrm{req}) - \bar{T}_\mathrm{model}(n,T_\mathrm{req})]^2} \qquad \bar{T}_\mathrm{model}(n,T_\mathrm{req})=\frac{1}{M}\sum_m T_\mathrm{model}(S_\mathrm{m},m,n,T_\mathrm{req}) \quad (5)$$

Since the model is well parametrized it is used to analyze the origin of the torque deviation (Fig. 6). Neglecting the influence of production uncertainty on the torque characteristic of the machine, one parameter set is found to fit all measured operating points of all machines. This parameter set S_* is found by minimizing the error e as sum across all M machines (6).

$$e(S_*) = \frac{1}{M}\sum_m e(m,S_*) \quad (6)$$

Fig. 10 shows the standard deviation as defined in (7) of the modeled torque for the 10 machines using the single parameter set S_* and therefore a model neglecting the influence of differences between the machines, i.e., without production uncertainty. The deviation σ_b is found to be larger than σ_a. This indicates that the variation of model parameters and therefore production differences have an influence on the torque characteristic.

$$\sigma_\mathrm{b}=\sqrt{\frac{1}{M}\sum_m [T_\mathrm{model}(S_*,m,n,T_\mathrm{req})- \bar{T}_\mathrm{model*}(n,T_\mathrm{req})]^2} \qquad \bar{T}_\mathrm{model*}=\frac{1}{M}\sum_m T_\mathrm{model}(S_*,m,n,T_\mathrm{req}) \quad (7)$$

To validate this, the modeled torque $T_\mathrm{model}(S_\mathrm{m},m,n,T_\mathrm{req})$ by using every parameter set $S_1 \ldots S_{10}$ is compared to the modeled torque $T_\mathrm{model}(S_*,m,n,T_\mathrm{req})$ using the deviation σ_c as defined in (8) which is shown in Fig. 11.

$$\sigma_\mathrm{c}=\sqrt{\frac{1}{M}\sum_m [T_\mathrm{model}(S_\mathrm{m},m,n,T_\mathrm{req})- T_\mathrm{model}(S_*,m,n,T_\mathrm{req})]^2} \quad (8)$$

The maximum value of σ_c of ≈ 1.1 Nm is reached at the maximum torque at rated speed. At the operating regions where a high deviation of torque was measured (σ_meas≈1.5 Nm) and modeled (σ_a≈1.6 Nm and σ_b≈2.0 Nm) only a small deviation of less than 0.7 Nm remains. The relative torque deviation is ≈ 1 % across the complete operating range.

No significant difference between the two series batches was found through the model parameters. The modeled torque from two machines of two batches do not differ significantly more than the modeled torque of two machines from a single batch.

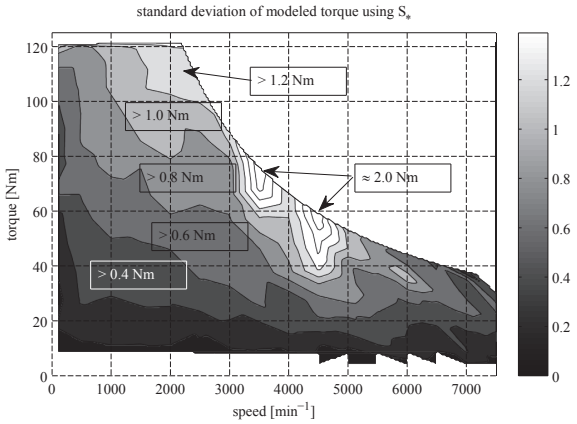

Fig. 10: Standard deviation σ_b of modeled torque using parameter set S_*.

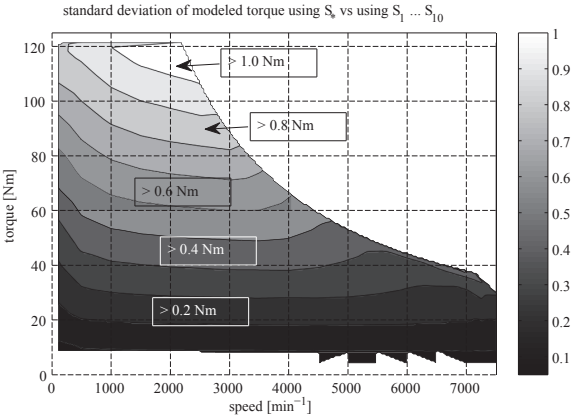

Fig. 11: Standard deviation σ_c of modeled torque using S_* and $S_1 \ldots S_{10}$.

VII. Disucussion

The torque deviation between the modeled torque using the best fitting parameter set for all machines S_* and best fitting parameter sets for every individual machine $S_1 \ldots S_{10}$ is about 1 % in the complete operating range. Therefore the influence of production uncertainty which is included in $S_1 \ldots S_{10}$ and neglected in S_* is assumed to create a relative torque uncertainty of approx. 1 %. On the other hand the measured torque deviation is with a maximum of 2.4 % somewhat higher than this. The reason for this higher deviation is the influence of the point of operation of the inverter. The inverter only estimates the rotor temperature and therefore cannot compensate completely for the actual rotor resistance. An increased torque accuracy could be achieved by implementing and parametrizing a better temperature model on the inverter of the machine.

VIII. Conlusions

Ten induction machines were characterized through off line and test bench measurements. An absolute torque error between requested torque and delivered torque of 6 Nm was found through these measurements. Deviations in the torque measurements of up to 2.4 % between the machines were found. A fundamental wave model was parametrized to fit the measured data for each machine best. Through these adapted parameter sets it is concluded that a part of the measured deviation is caused by the inverter. The torque deviation caused by production uncertainty of the induction machine is less than 1 % over the complete operating range. A more precise machine model to be parametrized in the inverter could increase the relative and absolute torque accuracy. If higher absolute or relative torque accuracy than 1 % is necessary, the inverter would additionally need machine parameters of every individual machine. No significant differences between the two series batches were found.

Acknowledgment

This paper was developed in the context of the co-operative project 'Mas:Stab', sponsored by the German Federal Ministry of Economic Affairs and Energy (BMWi), reference number 01MY12008A.

Federal Ministry
for Economic Affairs
and Energy

References

[1] Haksun Kim; Jiin Park; Kwangki Jeon; Sungjin Choi, "Integrated control strategy for torque vectoring and electronic stability control for in wheel motor EV," *2013 Proc. Conf. World Electric Vehicle Symposium and Exhibition (EVS27)*, pp.1,7, 17-20 Nov. 2013.

[2] Nandi, S.; Bharadwaj, R.M.; Toliyat, H.A., "Performance analysis of a three-phase induction motor under mixed eccentricity condition," *IEEE Transactions on Energy Conversion*, vol.17, no.3, pp.392,399, Sept. 2002.

[3] Tenhunen, A., "Calculation of eccentricity harmonics of the air-gap flux density in induction Machines by impulse method," *IEEE Transactions on Magnetics*, vol.41, no.5, pp.1904,1907, May 2005.

[4] Schlensok, C.; Hameyer, K., "Body-Sound Analysis of a Power-Steering Drive Considering Manufacturing Faults," *IEEE Transactions on Vehicular Technology*, vol.56, no.4, pp.1553,1560, July 2007.

[5] Young-Kyoun Kim; Jung-Pyo Hong; Jin Hur, "Torque characteristic analysis considering the manufacturing tolerance for electric machine by stochastic response surface method," *IEEE Transactions on Industry Applications*, vol.39, no.3, pp.713,719, May-June 2003.

[6] Gasparin, L.; Cernigoj, A.; Markic, S.; Fiser, R., "Additional Cogging Torque Components in Permanent-Magnet Motors Due to Manufacturing Imperfections," *IEEE Transactions on Magnetics*, vol.45, no.3, pp.1210,1213, March 2009.

[7] Arshad, W.M.; Kanerva, S.; Bono, S.; Menescardi, M.; Persson, H., "Medium-Large Induction Machines Starting Currents: Scaling Accuracy & Saturation Uncertainties," *IEEE Industry Applications Conference*, pp.2269,2276, 23-27 Sept. 2007.